Dalton Transactions

ROYAL SOCIETY OF CHEMISTRY

PAPER

View Article Online
View Journal | View Issue

Cite this: *Dalton Trans.*, 2023, **52**, 17993

ZIF-8 encapsulation improves the antifungal activity of benzaldehyde and methyl anthranilate in films†

Katia Caamaño, [a] Gracia López-Carballo, [b] Raquel Heras-Mozos, [b] Jana Glatz, [a] Pilar Hernández-Muñoz, [b] Rafael Gavara [b] and Mónica Giménez-Marqués *[a]

Received 2nd October 2023,
Accepted 8th November 2023

DOI: 10.1039/d3dt03229a

rsc.li/dalton

In this work, two ZIF-8-based biocomposites were obtained by entrapping the biomolecules benzaldehyde and methyl anthranilate *via* direct impregnation with fast encapsulation kinetics and high molecule payloads were achieved. The obtained biocomposites exhibit an enhanced antifungal activity against *Penicilium expansum* after integration in biopolymeric zein films in comparison with the action of free molecules, making these biomaterials promising candidates for food preservation and packaging applications.

Introduction

Fungal contamination in food leads to vast deterioration and a series of food safety problems. The effects of these microorganisms are related to cell growth, which can produce toxic secondary metabolites (mycotoxins) that besides the toxic effects frequently evolve to degenerative, toxinogenic, or carcinogenic issues. Fungi can also produce coloration or black points, not accepted by most consumers.[1] Among many strategies against fungal contamination, essential oils (EOs) and their derivatives, aromatic molecules extracted from plant components, have been investigated. Particularly, their incorporation into biopolymer films has a promising outlook as antimicrobials which are appealing in food-related applications.[2,3] EOs exhibit interesting physicochemical properties (*i.e.* antibacterial, antifungal, antiviral, pest control)[4] as natural products with high added values in terms of the environment and consumer demand. However, these compounds are susceptible to degradation by oxidation, volatilization or light exposure if not protected.[5] Indeed, direct incorporation of EOs within active packaging is limited and their encapsulation is needed in order to facilitate their application.

Nanostructured Metal–Organic Frameworks are presented as a viable tool to protect these fragile compounds. Their hybrid porous structures enable high loading of cargo and controlled release, which[6] make them appealing as cargo delivering nanocarriers in the agricultural field[7,8] as well as in the food industry to ensure the shelf-life of food products.[9,10] Indeed, the implementation of MOF-based composites into biofilms for the improvement of food preservation has been explored in the last few years resulting in sensing,[11,12] antibacterial[13,14] and antioxidant[15,16] performances. An archetypal MOF carrier used for these purposes is the zinc-based zeolitic imidazolate framework (ZIF) material known as ZIF-8, which exhibits permanent porosity (S_{BET} ~1600 m^2 g^{-1}), a high loading capacity and optimal thermal and chemical stability.[17] These characteristics linked with a facile synthesis, responsive behaviour,[18] and pH-sensitive degradation have positioned this material as a potential advanced platform for the controlled release of active molecules.[19] For instance, ZIF-8 has been utilised for the controlled delivery of fungicidal agents into plants for protection against diseases.[20] Taking into account these scaffold performances,[21,22] we aimed to explore the impact of incorporating ZIF-8 for the delivery of antifungal molecules supported on biopolymeric films.

In this work, two biomolecule@ZIF-8 biocomposites containing benzaldehyde (Bz) and methyl anthranilate (MA) have been prepared, and their fungicidal effect after integration into biopolymeric films has been analysed. Bz is the main constituent of bitter almond oil and is commonly employed as a flavouring agent with insecticidal, antioxidant, antibacterial, and antifungal activities[23,24] and has shown promising results for its use in active packaging.[25] MA can be naturally found in Concord and other *Vitis labrusca* grapes and has been extensively used as a flavouring agent in food and drugs, with a demonstrated antifungal activity.[26] Their direct incorporation

[a]*Instituto de Ciencia Molecular (ICMol), Universidad de Valencia, c/Catedrático José Beltrán 2, 46980 Paterna, Spain. E-mail: monica.gimenez-marques@uv.es*
[b]*Instituto de Agroquímica y Tecnología de Alimentos, IATA-CSIC, Av. Agustín Escardino 7, 46980 Paterna, Spain*

†Electronic supplementary information (ESI) available: Experimental details, methods and complementary physico-chemical characterization of the materials. See DOI: https://doi.org/10.1039/d3dt03229a

into ZIF-8 and simple processing into biofilms not only stabilizes and protects them, but also promotes an enhanced fungistatic and fungicidal activity, turning these biocomposites as a potential option for food packaging.

Results and discussion

Biomolecule encapsulation within ZIF-8 nanoparticles

The fungicidal Bz and MA molecules were encapsulated into preformed ZIF-8 nanoparticles (NPs) following a direct impregnation method previously developed (Fig. 1a).[9] ZIF-8 NPs were synthesised adapting a previously reported procedure,[27] obtaining NPs of *ca.* 100 nm (Fig. S1†). In a general procedure, ZIF-8 NPs were soaked into a Bz or MA aqueous ethanolic solution (20%) with a 5 : 1 biomolecule : ZIF-8 molar ratio. Biomolecule encapsulation was assessed by monitoring their concentration in the supernatant (calibration curves are displayed in Fig. S2†) by means of High-Performance Liquid Chromatography (HPLC), revealing a fast encapsulation kinetic profile where the concentration of the biomolecule drastically decreases after the first minute of contact and remains constant for 24 h (Fig. S3†). The gel-like solids (especially for MA@ZIF-8, Fig. S4†) were collected by centrifugation and air-dried. Part of the solid was thermally treated for further characterization.

FTIR analysis confirmed the presence of Bz and MA in the different biocomposites, as deduced from the detection of the most remarkable bands of the respective molecules in addition to the characteristic bands of ZIF-8 (Fig. 1b, c, Fig. S5†, Table S1†). Thermo-gravimetric analysis (TGA) of the obtained biocomposites was evaluated in comparison with the pristine ZIF-8 nanoMOF (Fig. 1d, e and Table S2†). To minimize the large solvent content remanent from the encapsulation media in the samples (especially for MA@ZIF-8, Fig. S6†), and facilitate the manipulation of the obtained materials, TGA profiles were carried out after preliminary thermal treatment. ZIF-8 NPs and Bz@ZIF-8 composite were pre-treated by heating at 100 °C for 3 hours. In the case of MA@ZIF-8, this thermal pre-treatment was extended up to 16 hours due to its gel nature. The Bz@ZIF-8 composite thermal profile exhibited the expected decomposition with an additional mass loss of *ca.* 21% up to 150 °C that can be related to the removal of benzaldehyde molecules (Bz boiling point is 178 °C). The MA@ZIF-8 thermal profile presents *ca.* 18% mass loss up to 100 °C related to departure of physisorbed solvent molecules. Between this temperature and 260 °C a distinctive mass drop of *ca.* 34% (dry base, D.B.) was detected, which can be assigned to the loss of encapsulated MA molecules (MA boiling point is 256 °C). Finally, the thermal stability of the ZIF-8 carrier was maintained in the composites, since the ligand decomposition temperature remained in the same range (± 5 °C) for all three materials. Therefore, considering the inorganic residue expected for ZIF-8 (*ca.* 36%), a molecule content of 21 and 34% was respectively estimated for Bz and MA biocomposites.

Framework integrity after biomolecule infiltration was evaluated by means of PXRD analysis performed before and after the encapsulation process, confirming the preservation of the ZIF-8 crystal structure in both cases (Fig. 1f). The relative intensity of the first diffraction peak corresponding to the (011) plane drastically decreases in both composite diffractograms, in good agreement with the increase of electronic density arising from the effective active molecule physisorption into the pores of the framework. However, the contribution to this intensity reduction due to an etching effect on the NPs' surface produced by the aldehyde molecules cannot be completely discarded.[28]

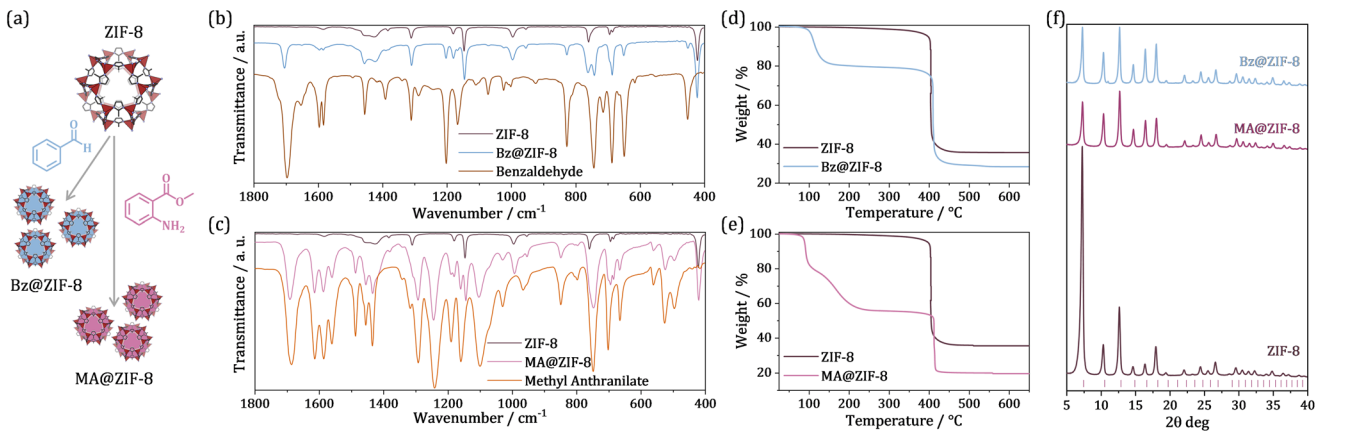

Fig. 1 (a) Scheme of biomolecule encapsulation into ZIF-8. (b–f) Characterization of the biomolecule@ZIF-8 composites as compared with ZIF-8: FTIR spectra of (b) Bz@ZIF-8 (blue) compared with ZIF-8 (purple) and benzaldehyde (yellow), and (c) MA@ZIF-8 (pink) compared with ZIF-8 (purple) and methyl anthranilate (orange). Thermo-gravimetric profiles of (d) Bz@ZIF-8 and (e) MA@ZIF-8, compared with the pristine ZIF-8 NPs. (f) XRPD patterns of the obtained biomolecule@ZIF-8 composites in comparison with pristine ZIF-8. The *hkl* reflection list of the ZIF-8 unit cell, obtained from crystallographic data,[17] is depicted at the bottom. All samples were dried at 100 °C for 3 h before measurement, except for MA@ZIF-8 which was dried for 16 h.

N_2 sorption studies before and after biomolecule encapsulation were carried out to evaluate the porosity of the composite materials and therefore assess the location of the active molecules (Fig. 2a). The control ZIF-8 material exhibits a type I(b) isotherm based on the IUPAC technical report,[29] where the abrupt increase of N_2 uptake in the low-pressure region is concordant with the microporosity of the material. An increase in the N_2 uptake is observed in the 0.9–1 region, related to the reduced particle size of the material, and expected characteristic filling of the inter-particular space. A porous surface decrease of *ca.* 84% and 90% was evidenced after Bz and MA encapsulation, respectively (S_{BET} = 1712 *vs.* 276 and 169 $m^2\ g^{-1}$ for ZIF-8 *vs.* Bz@ZIF-8 and MA@ZIF-8). A characteristic of ZIF-8 material is that exhibits flexibility upon gas uptake,[30] reflected in slope changes in the 0–0.1 P/P_0 region of the N_2 sorption isotherms. A close inspection of this gate-opening effect is displayed in the logarithmic representation of the N_2 adsorption branch (Fig. S7†), where three steps can be clearly distinguished. This gate opening behaviour of the ZIF-8 micropores is completely lost upon biomolecule infiltration, mainly due to a prevented reorientation of the imidazolate linkers upon gas sorption after biomolecule infiltration. Pore distribution analysis was conducted by employing the Horvath-Kawazoe equations for pore-size distribution (PSD).[31] Pristine ZIF-8 NPs present 3 PSD centres with 5.8, 7.4 and 9.4 Å. The two smaller PSD sites of ZIF-8 (Fig. 2b) are due to the flexible six-membered ring, and arise from the vibrations of the linker, as the rotation of the methylimidazolate ligand allows the infiltration of more N_2 molecules, expanding the available volume in the pore. Thus, the largest PSD centre of ZIF-8 nanoparticles, of about 9.4 Å, corresponds to the maximum opening available, almost the diameter of the ZIF-8 SOD cage.[32] In the composite materials, the largest pore drastically decreases, revealing an effective encapsulation of both molecules, which is also related to the loss of some degree of flexibility in the framework.

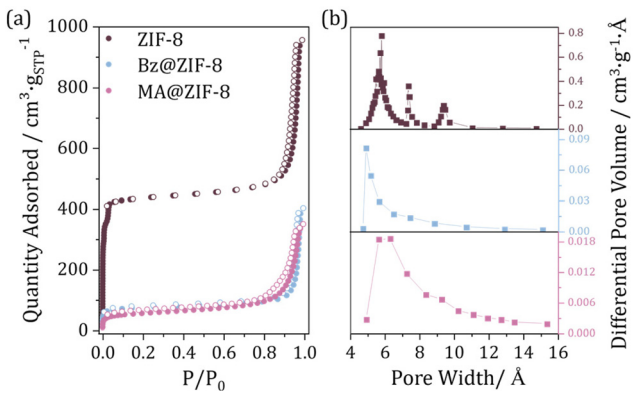

Fig. 2 (a) N_2 sorption isotherms at 77 K of Bz@ZIF-8 (blue) and MA@ZIF-8 (pink) compared with ZIF 8 (dark purple). Solid symbols for adsorption and open ones for desorption. Samples were activated at 100 °C for 3 h before measurement. (b) Pore size distributions were obtained employing the Horvath–Kawazoe equations of pristine ZIF-8 NPs and composites.

A more precise analysis of the biomolecule content in the composites was assessed by thermal desorption gas chromatography of the solids. A loading of *ca.* 31 and 33% was respectively obtained for the Bz and MA composites. A comparison of these loading values with other porous frameworks is presented in Table 1, revealing the high payload obtained in both ZIF-8-based composites. In view of these values and considering the inhibitory concentrations required for antifungal activity in essential oils,[33,34] it can be postulated that the loaded biomolecule contents obtained may be appropriate for fungicidal applications in both cases.

In vitro evaluation of antifungal activity

Microbiology studies were conducted to determine the efficiency of Bz@ZIF-8 and MA@ZIF-8 composites against *Penicilium expansum* after their integration in zein biopolymeric films and release of acive compounds. *P. expansum* was selected due to its spread spoilage activity causing blue mold decay of fruit and production of toxic secondary metabolites such as patulin and citrinin, resulting in an economic concern for the fresh fruit and the fruit processing industries.[35] Essentially, Bz and MA active molecules produce fungi inhibition when they are present at a concentration above the minimum inhibitory concentration. As soon as the concentration decreases below this limit, microorganisms resume their growth (fungistatic effect). When the concentration increases above the minimum lethal concentration, the microorganisms die, and they cannot grow even when the molecule concentration decreases to zero (fungicidal effect). Following a micro-atmosphere test, the fungal growth of *P. expansum* was monitored over 9 days (Fig. 3a, b and Fig. S8†). A drastic elimination of fungi was observed in the dish in contact with Bz@ZIF-8 for 9 days, with fungal growth being prevented even after the removal of the active layer. In contrast, the free benzaldehyde zein film retained *ca.* 90% size of the control growth after 48 h. Even though the growth rate was diminished over time compared to the control, fungal growth still reached 70% of the control at day 6 and remained constant after the removal of the active layer and monitoring at day 9. Similarly, no fungal presence could be observed in the dish in contact with the MA@ZIF-8 film and the fungal growth was still completely prevented after 9 days. These results reveal both fungistatic and fungicidal effects for the films containing Bz@ZIF-8 and MA@ZIF-8 composites. In the latter case, the free methyl anthranilate is already relatively effective, reducing *ca.* 75% of the fungal growth in the control plate after 48 h, increasing its

Table 1 Biomolecule loading in the composite materials determined by GC-MS in this work compared with other porous materials

Carrier	Loading/%	Ref.
ZIF-8 (Bz@ZIF-8)	31	This work
ZIF-8 (MA@ZIF-8)	33	
Nanoporous carbon based on MIL-101 (Bz)	56	36
γ-Cyclodextrin-based MOF (Bz)	3	37
NaY zeolite (MA)	34	38

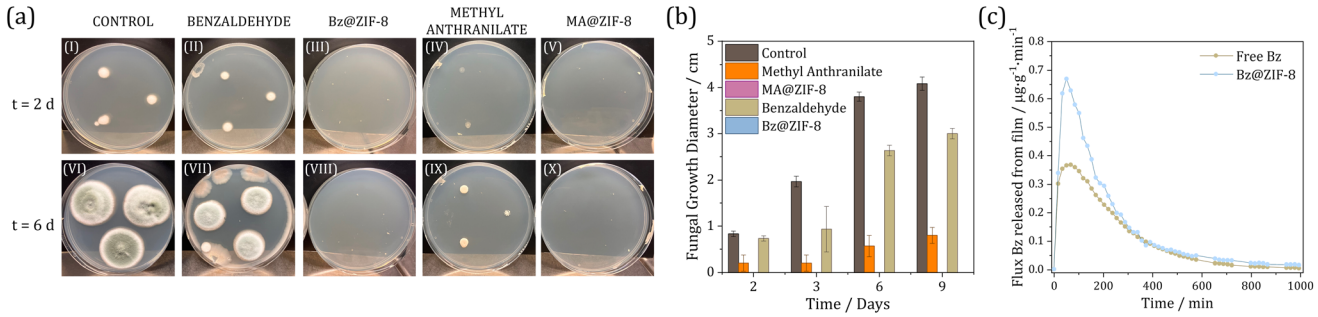

Fig. 3 (a) Images of the micro-atmosphere test carried out to determine the activity of Bz@ZIF-8 and MA@ZIF-8 containing films against *Penicilium expansum*: images of the Petri dishes showing 3 droplets of the fungal suspension for control (I, VI), free benzaldehyde(II, VII), Bz@ZIF-8 composite (III, VIII), free methyl anthranilate (IV, IX) and MA@ZIF-8 composite (V, X). The images of the Petri dishes on the top correspond to 48 hours of incubation whereas images on the bottom are taken, after 6 days. (b) Time evolution of the fungal growth diameter on the incubated dishes. (c) Flux evolution of Bz released from the films over time.

efficiency up to 85% after 6 days of incubation and maintaining this effect even after removal of the film.

This prolonged inhibition of the microorganisms during several days is explained by the retention of the active molecules in the headspace of the Petri dish where the *in vitro* test is carried out: the fungi are deposited over the culture media in the Petri dish and the film is attached to the Petri dish lid that covers the dish. Then, although the dish is not hermetically sealed, the released active compounds remain in the headspace after removal of the active layer.

Release kinetics of the films

To better understand the different behaviour of the free *vs.* encapsulated biomolecules, their release kinetics were studied by GC in conditions closed to that of a packaged food product (humid environment). During the release kinetics assay, the films were exposed to a stream of humid air that constantly removed out of the system the molecules released from the film and their liberation rate was quantified. In Fig. 3c, the evolution of Bz release from zein films is presented. Biomolecule release over time is significantly higher for the films containing Bz@ZIF-8 than for the films containing free Bz, though the release evolution follows a similar profile showing a maximum after 1 hour of exposure. This is most definitely a direct consequence of the greater concentration of Bz in the film, likely due to a prevented volatilization during the film manufacture, as revealed in the accumulated release of Bz (Fig. S9a†). Kinetically, the release is very similar, as can be seen in the insert, where the ratio of mass release at time "*t*" *vs.* the mass at infinite time has been plotted (Fig. S9b†). Such analysis on MA could not be carried out, as the low volatility of this substance resulted in concentrations below the sensitivity of the technique. Nevertheless, the improvement in antifungal capacity for MA@ZIF-8 composites may also be associated with an efficient incorporation into the film. Thus, it can be established that Bz and MA encapsulation into ZIF-8 and later incorporation within the films improves the antifungal performance, revealing both fungistatic and fungicidal effects.

Experimental

Materials and methods

Materials. Zinc nitrate hexahydrate (98%) and 2-methylimidazole (98%) were purchased from Sigma-Aldrich. Benzaldehyde (BA) (99%+) was purchased from Alfa Aesar. Methyl anthranilate (MA) was purchased from Sigma-Aldrich. Methanol and absolute ethanol were purchased from Honeywell. All chemicals were used as received without the need of further purification and Milli–Q water was obtained from a Millipore Milli–Q system.

Synthesis of ZIF-8 nanoparticles. ZIF-8 NPs were synthesized at 60 °C adapting the procedure described by Langner and coworkers.[27] A solution of $Zn(NO_3)_2{\cdot}6H_2O$ (1.476 g, 5 mmol) in 100 mL of methanol at 40 °C was rapidly added to a solution of 2-methylimidazole (3.286 g, 40 mmol) in 50 mL of methanol at the same temperature. The mixture was heated at 65 °C and stirred for 1 h before placing the flask in an ice bath to stop the reaction. The precipitate was isolated by centrifugation (8228*g*, 30 min, room temperature), washed with methanol three times, and dried in air overnight.

Preparation of biomolecule@ZIF-8 composite materials. Bz@ZIF-8 and MA@ZIF-8 composites were obtained adapting a direct impregnation method.[9] In a typical preparation, 11.65 mL of benzaldehyde or 16.61 mL of methyl anthranilate emulsions (20 mg mL^{-1} concentration) prepared in a H_2O : EtOH (4 : 1) mixture were directly added to 100 mg of dried ZIF-8 NPs. After 1 h stirring in a 360° rotating shaker, the biomolecule@ZIF-8 materials were retrieved by centrifugation (12 857*g*, 20 min) and dried in air overnight. The composites were then dried at 100 °C in an oven for 3 or 16 hours, respectively for Bz@ZIF-8 and MA@ZIF-8.

Determination of encapsulation kinetics. Calibration curves were prepared and measured using an HPLC 1260 Agilent Infinity equipment with UV-vis detection. Benzaldehyde and methyl anthranilate solutions were prepared in acetonitrile in the range of 0.015 to 0.2 and 0.25 to 5 mg mL^{-1}, respectively. The column used was 150 × 4.6 mm packed with 4 μm particles of C18 (Agilent) operated at 25 °C. To elute the bio-

molecules, the mobile phase employed was a binary mix of acetonitrile (70%) and water. The flow rate of the mixture was fixed at 1 mL min^{-1}, and the injection volume of the samples was 20 μL. The molecules were detected by UV-vis at λ = 260 nm for benzaldehyde and at λ = 250 nm for methyl anthranilate with retention times of 2.04 and 3.55 min, respectively. To ensure the reproducibility, calibration curves were repeated 6 times. Benzaldehyde and methyl anthranilate concentration in the encapsulation supernatant was analysed between one minute and seven days. Each encapsulation was performed in triplicate to ensure the reproducibility.

Determination of the loading capacity (LC). Bioactive molecule content in the composites was determined by thermal desorption gas chromatography, using an HP 7890B equipped with an HP5 column of 30 m, 320 μm of diameter and 0.25 μm of thickness. The thermal gradient employed was: 40 °C (3 min), 10 °C min^{-1} ramp until 200 °C and 15 min isotherm. A 1 mg sample was placed and weighed in an ultra-inert microvial (Agilent Technologies) and kept in the injector holder. The multimodal injector, used in thermal desorption mode, was heated on a ballistic ramp (600 °C min^{-1}) from 40 to 200 °C in a 4 min isotherm fully desorbing volatile molecules into the column, and the detector was set at 220 °C. The instrument was calibrated by injecting known concentrations of benzaldehyde and methyl anthranilate.

Biomolecule loading in the obtained composite materials was quantified and expressed according to the following equation:

$$\text{Biomolecule loading \%} = \frac{\text{mass of biomolecule}}{\text{mass of composite}} \times 100$$

Characterization of ZIF-8 NPs and biomolecule@ZIF-8 composite materials. Particle size measured as the hydrodynamic diameter in methanolic suspensions was collected on Zetasizer Ultra equipment operating at 25 °C, equipped with a red (633 nm) laser and an avalanche photodiode detector (Malvern, UK). X-ray powder diffraction patterns were acquired using an X-ray diffractometer (PANalytical Empyrean) with copper as the radiation source (Cu-Kα, 1.5418 Å). Infrared spectroscopy was conducted employing an ALPHA II FTIR spectrometer (Bruker). Thermogravimetric analyses were carried out with TGA 550 (TA Instruments) in high-resolution mode (Ramp: 20.0 °C min^{-1} to 700 °C; Res 4 Sensitivity 3). N_2 sorption isotherms were obtained using a TRISTAR II apparatus (Micromeritics) at −196 °C. All samples were activated before TGA and sorption measurements at 100 °C for 3 or 16 hours, respectively for Bz@ZIF-8 and MA@ZIF-8 composites.

Preparation of polymeric films. Two zein films were prepared from an 80% hydroalcoholic solution containing 15% weight of zein. Two fractions were separated: to the first one 0.5 g biomolecule@ZIF-8 composite was added per g of zein, whereas the corresponding amount of free biomolecule (considering the loading capacity) was directly added to the second fraction. The mixtures were spread on a flat surface of PTFE using a 100 μm coating rod and dried in an open oven at 75 °C for 10 min. The films obtained were stored in PP/met envelopes until further characterization. The residual content of biomolecule in both films was analysed. For this, the samples were cut from both films, introduced into a micro vial, and tested by thermal desorption and gas chromatography obtaining a final concentration of biomolecule of 0.150 ± 0.015 and 0.165 ± 0.020 g g^{-1} for benzaldehyde and methyl anthranilate in the encapsulated film, and 0.105 ± 0.011 and 0.155 ± 0.020 g g^{-1} in the film with pure benzaldehyde and methyl anthranilate, respectively.

Release kinetics. Relative release evolution and cumulative release profiles were measured by monitoring the benzaldehyde release from the polymeric films at 23 ± 1 °C and 95 ± 3% RH (simulating the exposure to fresh food). A piece of sample of the film was placed on a desorption tube where a humid 15 mL min^{-1} stream of N_2 hauled the released product into the injector of a gas chromatograph (using a heated conduction at 70 °C to avoid condensation). Humidity and gas flow rate were controlled by using a thermohygrometer (Reptiles planet, Saint Jean de Védas France), and an Aalborg GFM-1700 mass flowmeter (Sigma-Aldrich), respectively. The benzaldehyde release flow was determined using an HP7890 gas chromatograph with a 200 μL automatic injection valve and an HP5 column of 30 m, 320 μm diameter, and 0.25 μm thickness. Thermal conditions were as follows: 80 °C at the injection valve, 200 °C at the injection port, 220 °C at the flame ionization detector, and 100 °C at the column oven.

Determination of fungicidal activity. The strain of *Penicillium expansum* fungus was obtained from the Spanish collection of type cultures (CECT 2278). The fungus was grown on agar before the experiment in PDA (potato dextrose agar) medium – which is a solid general fungal growth medium. The fungus grew for seven days at 28 °C, until the entire plate was covered (90 mm). In this phase the spores were extracted. The extracting protocol consisted of the following steps: in a laminar flow cabinet 10 mL of peptone water with Tween 80 (0.05%) were dropped on the surface of the plate and the mycelium was broken by scraping with the help of a spatula. 5 mL of the formed suspension were shaken vigorously with a vortex. After serial dilutions a concentration of 10^5 spores per mL was achieved – the spores were counted in an optical microscope with the help of a Neubuer camera. 3 μL of the said suspension were placed equidistantly on the PDA plate. A film containing either the biomolecule@ZIF-8 composite or the equivalent content of free active molecule was placed on the inside of the Petri dish lid. The prepared dishes were incubated at 28 °C and the growth of the fungus was monitored visually by measuring the growth halo. After six days of incubation the films were removed, and the incubation of the plates was continued until day 9.

Conclusions

In this work, two ZIF-8-based biocomposites containing benzaldehyde and methyl anthranilate were obtained employing a direct infiltration method. The encapsulation kinetics revealed

an immediate encapsulation process, with loadings of *ca.* 20–30 wt%. The obtained composites Bz@ZIF-8 and MA@ZIF-8 were implemented into biopolymeric zein films and tested in antifungal activity essays. The released benzaldehyde and methyl anthranilate dose was high enough to oppose fungal growth over 9 days revealing an improved fungistatic and fungicide activity, as compared to the "free" biomolecule integrated in the biopolymeric films. These results evidence that the prepared biomolecule@ZIF-8 composites are potential candidates for food packaging applications due to their direct preparation, simple processing, and a scaffold-mediated efficient incorporation that enhances antifungal action.

Conflicts of interest

There are no conflicts to declare.

Acknowledgements

This work has been supported by grants TED2021-132729A-I00, PID2020-118564GA-I00, PID2021-123077OB-I00 and CEX2019-000919-M, funded by MCIN/AEI/10.13039/501100011033, EU NextGenerationEU/PRTR and by Generalitat Valenciana (PROMETEO CIPROM/2022/48). M. G.-M. thanks MICINN for a Ramón y Cajal (RYC2019-027902-I), K. C. for a PRE2018-083355 grant included in Project MAT2017-89993-R funded by "ERDF A way of making Europe".

References

1 N. N. Van Long and P. Dantigny, *Fungal Contamination in Packaged Foods*, Elsevier Inc., 2016.
2 R. Ribeiro-Santos, M. Andrade, N. R. de Melo and A. Sanches-Silva, *Trends Food Sci. Technol.*, 2017, **61**, 132–140.
3 A. Acevedo-Fani, L. Salvia-Trujillo, M. A. Rojas-Graü and O. Martín-Belloso, *Food Hydrocolloids*, 2015, **47**, 168–177.
4 S. Tariq, S. Wani, W. Rasool, K. Shafi, M. A. Bhat, A. Prabhakar, A. H. Shalla and M. A. Rather, *Microb. Pathog.*, 2019, **134**, 103580.
5 B. Prakash, A. Kujur, A. Yadav, A. Kumar, P. P. Singh and N. K. Dubey, *Food Control*, 2018, **89**, 1–11.
6 M. Shen, F. Forghani, X. Kong, D. Liu, X. Ye, S. Chen and T. Ding, *Compr. Rev. Food Sci. Food Saf.*, 2020, **19**, 1397–1419.
7 M. Anstoetz, T. J. Rose, M. W. Clark, L. H. Yee, C. A. Raymond and T. Vancov, *PLoS One*, 2015, **10**, 1–16.
8 S. Rojas, A. Rodríguez-Diéguez and P. Horcajada, *ACS Appl. Mater. Interfaces*, 2022, **14**, 16983–17007.
9 K. Caamaño, R. Heras-Mozos, J. Calbo, J. C. Díaz, J. C. Waerenborgh, B. J. C. Vieira, P. Hernández-Muñoz, R. Gavara and M. Giménez-Marqués, *ACS Appl. Mater. Interfaces*, 2022, **14**, 10758–10768.
10 H. Wang, E. Lashkari, H. Lim, C. Zheng, T. J. Emge, Q. Gong, K. Yam and J. Li, *Chem. Commun.*, 2016, **52**, 2129–2132.
11 N. Huo, D. Li, S. Zheng and W. Deng, *Chem. Eng. J.*, 2022, **432**, 134317.
12 Z. Riahi, A. Khan, J. W. Rhim, G. H. Shin and J. T. Kim, *Int. J. Biol. Macromol.*, 2023, **249**, 126040.
13 J. Zhao, F. Wei, W. Xu and X. Han, *Appl. Surf. Sci.*, 2020, **510**, 145418.
14 Y. Liang, Y. Yao, Y. Liu, Y. Li, C. Xu, L. Fu and B. Lin, *Int. J. Biol. Macromol.*, 2022, **214**, 181–191.
15 A. Sultana, L. Kumar and K. K. Gaikwad, *Int. J. Biol. Macromol.*, 2023, **243**, 125031.
16 L. Y. Maroufi, N. Shahabi, A. A. Fallah, E. Mahmoudi, M. H. Al-Musawi and M. Ghorbani, *Int. J. Biol. Macromol.*, 2023, **250**, 126176.
17 K. S. Park, Z. Ni, A. P. Cote, J. Y. Choi, R. Huang, F. J. Uribe-Romo, H. K. Chae, M. O'Keeffe and O. M. Yaghi, *Proc. Natl. Acad. Sci. U. S. A.*, 2006, **103**, 10186–10191.
18 C. Carrillo-Carrión, R. Martínez, M. F. Navarro Poupard, B. Pelaz, E. Polo, A. Arenas-Vivo, A. Olgiati, P. Taboada, M. G. Soliman, Ú. Catalán, S. Fernández-Castillejo, R. Solà, W. J. Parak, P. Horcajada, R. A. Alvarez-Puebla and P. del Pino, *Angew. Chem.*, 2019, **131**, 7152–7156.
19 S. Feng, X. Zhang, D. Shi and Z. Wang, *Front. Chem. Sci. Eng.*, 2021, **15**, 221–237.
20 W. Liang, Z. Xie, J. Cheng, D. Xiao, Q. Xiong, Q. Wang, J. Zhao and W. Gui, *ACS Nano*, 2021, **15**, 6987–6997.
21 Y. Hara, M. E. Castell-Perez and R. G. Moreira, *J. Food Sci.*, 2023, **88**, 2512–2522.
22 A. Khezerlou, M. Tavassoli, M. Alizadeh-sani, M. Hashemi, A. Ehsani and S. Punia, *Int. J. Biol. Macromol.*, 2023, **251**, 126334.
23 I. Ullah, A. L. Khan, L. Ali, A. R. Khan, M. Waqas, J. Hussain, I. J. Lee and J. H. Shin, *J. Microbiol.*, 2015, **53**, 127–133.
24 J. H. Kim, K. L. Chan, N. Mahoney and B. C. Campbell, *Ann. Clin. Microbiol. Antimicrob.*, 2011, **10**, 23.
25 H. Calvo, I. Mendiara, E. Arias, A. P. Gracia, D. Blanco and M. E. Venturini, *Postharvest Biol. Technol.*, 2020, **166**, 111208.
26 A. H. Chambers, S. A. Evans and K. M. Folta, *J. Agric. Food Chem.*, 2013, **61**, 12625–12633.
27 C. W. Tsai and E. H. G. Langner, *Microporous Mesoporous Mater.*, 2016, **221**, 8–13.
28 H. Shen, H. Zhao, E. Benassi, L. Chou and H. Song, *CrystEngComm*, 2023, **25**, 3308–3316.
29 M. Thommes, K. Kaneko, A. V. Neimark, J. P. Olivier, F. Rodriguez-Reinoso, J. Rouquerol and K. S. W. Sing, *Pure Appl. Chem.*, 2015, **87**, 1051–1069.
30 D. Fairen-Jimenez, S. A. Moggach, M. T. Wharmby, P. A. Wright, S. Parsons and T. Düren, *J. Am. Chem. Soc.*, 2011, **133**, 8900–8902.
31 S. U. Rege and R. T. Yang, *AIChE J.*, 2000, **46**, 734–750.
32 X. Mei, S. Yang, P. Lu, Y. Zhang and J. Zhang, *Front. Chem.*, 2020, **8**, 1–10.

33 A. Aragón-Gutiérrez, R. Heras-Mozos, A. Montesinos, M. Gallur, D. López, R. Gavara and P. Hernández-Muñoz, *Polymers*, 2022, **14**, 3405.
34 R. Heras-Mozos, R. Gavara and P. Hernández-Muñoz, *Carbohydr. Polym.*, 2022, **283**, 119137.
35 L. Yu, N. Qiao, J. Zhao, H. Zhang, F. Tian, Q. Zhai and W. Chen, *Food Biosci.*, 2020, **36**, 100633.
36 C. J. Wu, Y. F. Liu, W. F. Zhang, C. Zhang, G. B. Chai, Q. D. Zhang, J. Mao, I. Ahmad, S. S. Zhang and J. P. Xie, *Colloids Surf., A*, 2022, **640**, 128453.
37 B. Zhang, H. Chen, Q. Hu, L. Jiang, Y. Shen, D. Zhao and Z. Zhou, *Adv. Funct. Mater.*, 2021, **31**, 2105395.
38 S. P. G. Costa, O. S. G. P. Soares, C. A. Aguiar and I. C. Neves, *Ind. Crops Prod.*, 2022, **187**, 115397.